Balmer-line emission from low-energy H$^+$ impact on rare-gas atoms

B. Van Zyl, M. W. Gealy, and H. Neumann

Department of Physics, University of Denver, Denver, Colorado 80208

Absolute cross sections for the emission of Balmer-α radiation have been measured for low-energy H$^+$ impact on He, Ne, Kr, and Xe atoms. Measurements were made at H$^+$ energies of 2.0 and 1.25 keV for He, from 2.0 to 0.5 keV for Ne, and from 2.0 to 0.04 keV for Kr and Xe. The Balmer-β emission cross sections were also measured for Kr and Xe, as were the polarizations of the radiations, and the contributions to the radiations from decay of the $3s$ and $4s$ excited states of hydrogen were resolved for H$^+$ energies above 0.2 keV. The data are compared with similar results for Ar reported earlier, and with the results of other workers at higher H$^+$ energies.

I. INTRODUCTION

In an earlier paper,[1] the absolute cross sections and polarizations for emission of Balmer-α (H$_\alpha$) and Balmer-β (H$_\beta$) radiations resulting from H$^+$ + Ar collisions were reported. These emissions, caused by electron capture by the fast H$^+$ into the $n = 3$ and 4 levels of hydrogen, were measured for H$^+$ energies from 2.0 down to 0.04 keV. For H$^+$ energies above 0.2 keV, the H$_\alpha$ and H$_\beta$ emissions coming from the $3s \rightarrow 2p$ and $4s \rightarrow 2p$ hydrogenic transitions, respectively, were separated from the other $np \rightarrow 2s$ and $nd \rightarrow 2p$ emission components. This was accomplished by observing the growth of the photon signals as a function of distance into the target cell, and employing an analysis based upon the relatively long radiative lifetimes of these excited ns states.[2]

This paper reports similar data for H$^+$ impact on Kr and Xe targets. The experimental techniques used to make the measurements were identical with those employed earlier for Ar targets,[1,3] and will not be reviewed here. As before, measurements were made as a function of target-cell pressure to isolate the photon signals of interest from those caused by second-collision effects occurring along the projectile-beam path through the target cell. The absolute calibration of the photon detector employed[3] can be traced again to the accurately known cross sections for $n\,^1S \rightarrow 2\,^1P$ emissions resulting from electron-impact excitation of He atoms.[4]

H$_\alpha$ emissions resulting from H$^+$ collisions with He and Ne targets were also observed. However, because of the small magnitudes of the photon signals, their rapid decrease with decreasing H$^+$ energy, and other sources of photon signal present in the target cell, definitive cross-section measurements could not be made for H$^+$ energies below 1.25 keV for He targets and 0.5 keV for Ne targets. Even here, it was not possible to separate accurately the various emission components or to measure the radiation polarizations.

II. H$^+$ IMPACT ON He AND Ne

The reactions leading to population of the $3s$, $3p$, or $3d$ excited states of hydrogen by H$^+$ impact on He or Ne targets are highly endothermic (~ 23 eV for He and ~ 19 eV for Ne). Thus it is not surprising that these H$_\alpha$ emission cross sections should have small magnitudes in the range of low H$^+$ energies investigated here. This fact by itself, however, did not prevent an accurate measurement of these emission cross sections at very low H$^+$ energies. Rather, the measurement difficulties stemmed from two other sources of photon signals in the target cell.

First, the "effective" H$_\alpha$ emission cross section for H$^+$ impact on the residual-gas particles present in the target cell (presumably mostly water and hydrocarbon molecules) at about 10^{-7} Torr pressure was found to be more than 4 orders of magnitude larger than that for, say, H$^+$ + He collisions for H$^+$ energies below 1 keV. Thus, even though the He pressure in the target cell could be raised up to 10^4 times this residual-gas pressure, most of the photon signal still came from H$^+$ impact on these residual-gas targets. Second, the H$_\alpha$ emission cross section for neutral H impact on He is more than 3 orders of magnitude larger than that for H$^+$ impact.[5] As a consequence, conversion of only a small fraction of the H$^+$ moving through the target cell into H via electron-capture reactions resulted in a very large increase in the measured H$_\alpha$ signal from secondary H + He collisions, and prevented meaningful operation of the target cell at high He pressures. These problems were somewhat less severe for Ne targets, although the H$_\alpha$ emission cross section for H + Ne collisions[6] is still much larger than that for H$^+$ impact.

While these problems were also present at higher H$^+$ energies, the photon signals from the reactions of interest were sufficiently large here to allow their approximate determination by careful examination and extrapolation of the total measured signals as functions of the He and Ne target-cell pressures. The results of these analyses give the total H$_\alpha$ emission cross-section values shown in Table I. As can be seen, these values are indeed small, but do tend to scale with the square of the H$^+$ energy, as expected for such highly nonresonant electron-capture processes at low ion energies.[7]

While the fraction of these emissions resulting from the $3s \rightarrow 2p$ transition could not be determined accurately, a value of 0.45 ± 0.20 was typical of the data. This value is

TABLE I. H_α emission cross sections for H^+ impact on He and Ne targets.

H^+ energy (keV)	Cross section He targets	$(10^{-20}$ cm$^2)$ Ne targets
2.00	1.6±0.6	16.1±5.6
1.25	0.6±0.3	6.3±2.2
0.80		1.7±0.9
0.50		1.1±0.7

quite close to the value of 0.47 expected if the 3s, 3p, and 3d excited states of hydrogen were populated equally in the electron-capture process.[2]

Attempts were also made to observe H_β emission from these reactions. While the data for $H^+ + He$ collisions were of no quantitative value, those for $H^+ + Ne$ collisions did suggest a total H_β emission cross section about an order of magnitude smaller than that for H_α emission, and having a similar H^+ energy dependence.

III. H^+ IMPACT ON Kr AND Xe

The total H_α and H_β emission cross sections resulting from H^+ impact on Kr and Xe targets are shown in Figs. 1 and 2, respectively. Also shown are the components of these total emissions resulting from decay of the excited hydrogenic states indicated for H^+ energies above 0.2
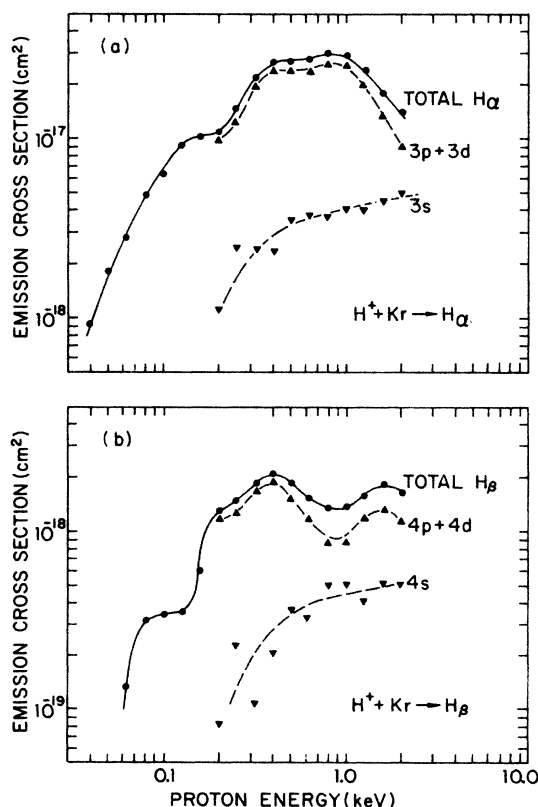

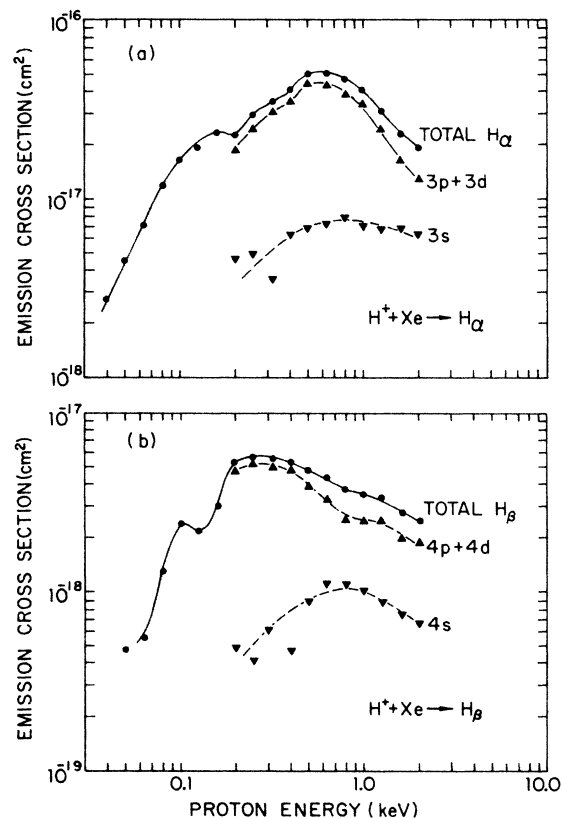FIG. 2. H_α and H_β emission cross sections for $H^+ + Xe$ collisions.

FIG. 1. H_α and H_β emission cross sections for $H^+ + Kr$ collisions.

keV. The uncertainties in the total emission and the $(np \rightarrow 2s) + (nd \rightarrow 2p)$ emission cross sections are typically less than ±15%, except for H_β emission from Xe targets. Here, some of the observed photon signal may have come from the 486.2-nm emission line of Xe^+, which would be transmitted by the interference filter used to isolate H_β emission.[3] For H^+ energies above 0.5 keV, the $ns \rightarrow 2p$ emission cross sections are uncertain by about ±25%, but become increasingly uncertain at lower H^+ energies.

As can be seen, these emission cross sections are richly structured, reflecting the considerable complexities of the interactions involved. Further evidence of these complexities is shown in Figs. 3 and 4, where the polarizations of the emitted radiations are plotted.[8] (The uncertainties in polarization are typically less than ±0.02 for H^+ energies above 0.06 keV.) These polarization data suggest that the relative populations of the various m_l substates of the np and nd states produced in the collisions[2,9] depend strongly on H^+ energy. It seems plausible that the structures in both the cross-section and polarization data result from interference between the various interaction channels leading to these emissions.

While the details of these interaction mechanisms have not been identified, the earlier paper on $H^+ + Ar$ collisions[1] contained considerable discussion about various possibilities. Because Kr and Xe are electronically similar to Ar, the same general types of interactions should occur for these atoms, so this discussion will not be repeated here. It should be noted, however, that the relative effi-
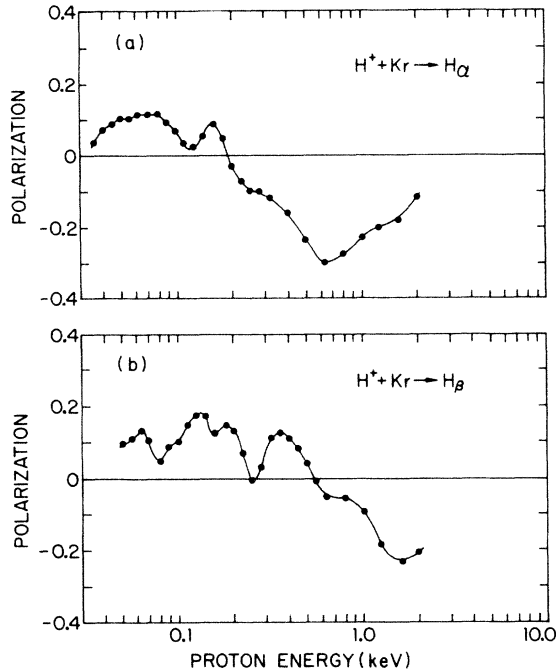
FIG. 3. Polarizations of H$_\alpha$ and H$_\beta$ radiations from H$^+$ + Kr collisions.

ciencies of the interaction channels discussed may be influenced by the lower ionization potentials of Kr and Xe relative to Ar.

It was also suggested in Ref. 1 that the particular reaction channel H$^+$ + Ar→H$^-$ + Ar^{2+}→H* + Ar$^+$ may play an important role in excited hydrogen-atom formation in such collisions. Here, the strongly bound Coulomb state is populated early in the collision (either directly or via
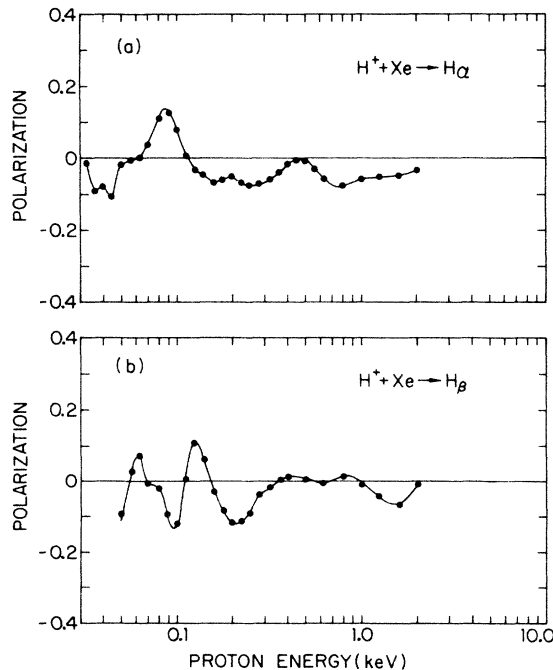

FIG. 4. Polarizations of H$_\alpha$ and H$_\beta$ radiations from H$^+$ + Xe collisions.

the H$^+$ + Ar→H + Ar$^+$ precursor reaction) and (diabatically) crosses and feeds the various states leading to H* formation on the outward leg of the collision. Again, similar reaction channels are available to the H$^+$ + Kr and H$^+$ + Xe systems. Indeed, for H$^+$ + Xe collisions, Jaecks and Martin[10] have found that the outgoing channels leading to H$^-$, H$^*(2s)$, and H$^*(2p)$ formation all appear to be coupled. If this is so, the channels leading to the higher-lying nl states may also share this ancestry.

IV. DATA COMPARISONS AND DISCUSSION

Figures 5—9 compare the H$_\alpha$ emission cross sections reported here (and the earlier results[1] for Ar) for He through Xe targets, respectively, with higher-energy data of other workers.[11] The comparisons are made for H$^+$ energies from 0.2 to 200 keV. The solid symbols connected by the solid curves are the total H$_\alpha$ emission cross sections, while the open symbols connected by the dashed curves are the emission cross sections from the $3s \rightarrow 2p$ transition. Because the branching ratio for this transition is unity, and cascade population of the $3s$ state from higher-lying np states is small (these states decaying preferentially to the $1s$ and $2s$ states), the dashed curves are essentially the cross sections for electron capture into the $3s$ state of hydrogen.

The data of Lenormand[12] for all targets and those of Ford and Thomas[13] for He and Ar targets are plotted as published. The results of Hughes et $al.$[14] for He, Ne, and Ar targets are shown as dotted curves, the upper curve being for total H$_\alpha$ emission and the lower curve being for the $3s \rightarrow 2p$ emission component. The relative cross-section measurements of Dawson and Loyd[15] for He, Ar, and Kr targets, which were normalized to older results of Hughes et $al.$,[16] have been renormalized here, as will be discussed below. All the other data shown represent abso-
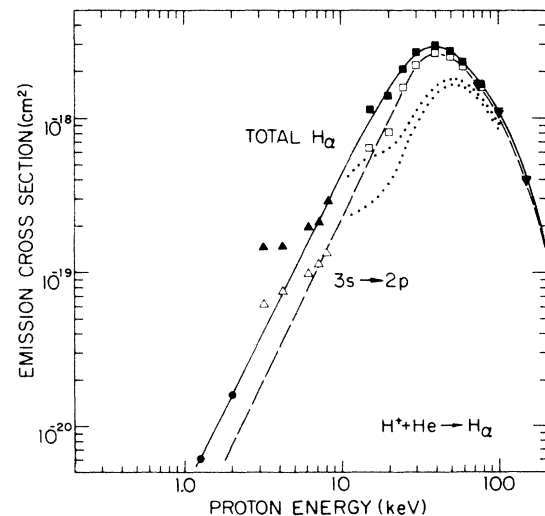

FIG. 5. H$_\alpha$ emission cross sections for H$^+$ + He collisions. Data sources: ●, present results; ■,□, Lenormand (Ref. 12); ▼, ▽, Ford and Thomas (Ref. 13); · · · ·, Hughes et $al.$ (Ref. 14); and ▲,△, adjusted results (see text) of Dawson and Loyd (Ref. 15).
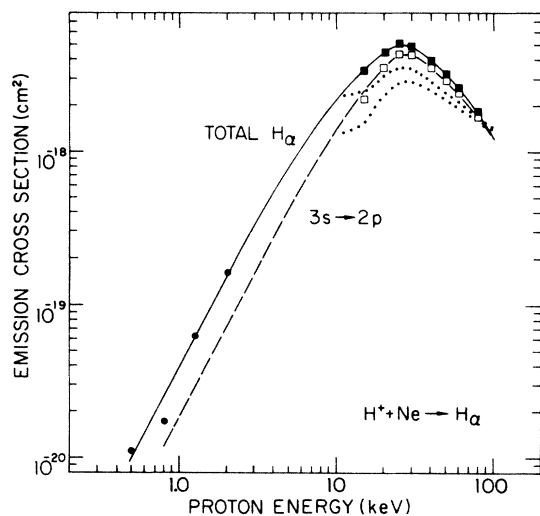
FIG. 6. H_α emission cross sections for $H^+ + Ne$ collisions. Data sources: ●, present results; ■,□, Lenormand (Ref. 12); and · · · ·, Hughes *et al.* (Ref. 14).
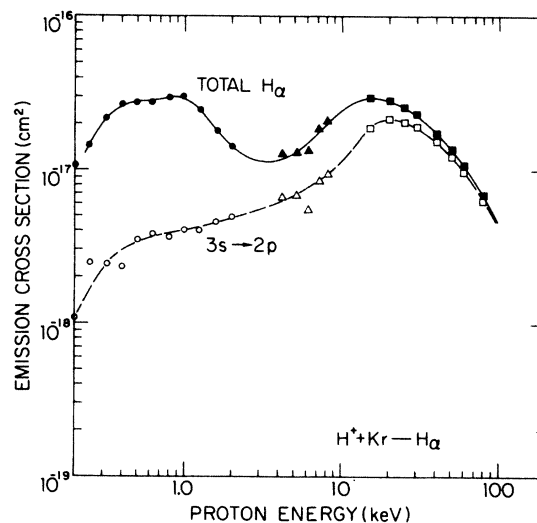
FIG. 8. H_α emission cross sections for $H^+ + Kr$ collisions. Data sources: ●,○, present results; ■,□, Lenormand (Ref. 12); and ▲,△, adjusted results (see text) of Dawson and Loyd (Ref. 15).

lute measurements, each employing an independent absolute photon-detector calibration.

The total H_α emission data of Lenormand[12] for He targets shown in Fig. 5 are in good agreement with those of Ford and Thomas[13] at high H^+ energies, and can be connected smoothly to the present low-energy results with a cross-section curve having an E^2 energy dependence.[7] The data of Dawson and Loyd[15] at 8.2 and 7.2 keV H^+ energy have been normalized to this curve by multiplying their published results by 0.467. With this normalization, the $3s \rightarrow 2p$ emission cross sections measured by all these workers can be joined smoothly with the approximate

value of 0.45 times the total H_α emission cross section obtained here (see Sec. II).

The renormalized data of Dawson and Loyd[15] at H^+ energies of 4.2 and 3.2 keV are in poor agreement with the curves drawn in Fig. 5. However, it seems possible[17] that these results may have been affected by the kinds of measurement problems discussed in Sec. II, which would cause larger measured cross-section values. The data of Hughes *et al.*[14] shown in Fig. 5 are discussed below.

The data of Lenormand[12] for Ne targets in Fig. 6 can again be connected to the present data using a curve with an E^2 energy dependence. As for He targets, the $3s \rightarrow 2p$ emission cross section has been set to 0.45 of the total H_α emission cross section at low H^+ energies. Again, the re-
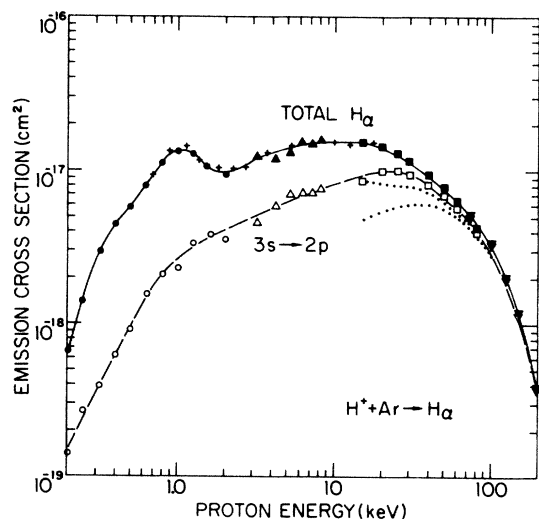

FIG. 7. H_α emission cross sections for $H^+ + Ar$ collisions. Data sources: ●,○, Van Zyl *et al.* (Ref. 1); ■,□, Lenormand (Ref. 12); ▼,▽, Ford and Thomas (Ref. 13); · · · ·, Hughes *et al.* (Ref. 14); ▲,△, adjusted results (see text) of Dawson and Loyd (Ref. 15); and +, adjusted results (see text) of Suchannek and Sheridan (Ref. 18).

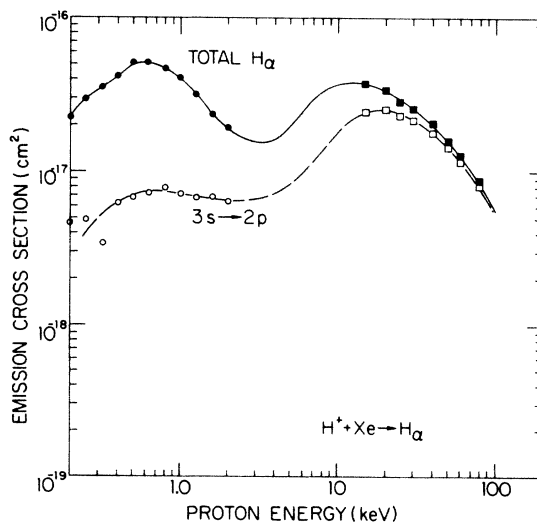FIG. 9. H_α emission cross sections for $H^+ + Xe$ collisions. Data sources: ●,○, present results; and ■,□, Lenormand (Ref. 12).

sults of Hughes et al.[14] are discussed below.

The data for Ar targets are presented in Fig. 7, where the present results are from Van Zyl et al.[1] The results of Lenormand[12] again agree with those of Ford and Thomas[13] at high H$^+$ energies, and the total H$_\alpha$ emission cross section can be joined with the present low-energy data by the solid curve drawn. The dependence of this curve on H$^+$ energy from 2 to 15 keV was deduced from the data of Suchannek and Sheridan.[18]

Suchannek and Sheridan[18] measured an "apparent" H$_\alpha$ emission cross section at 4.7 cm into their target cell. Because of the long radiative lifetime of the 3s state of hydrogen (1.6×10^{-7} sec), much of the $3s \rightarrow 2p$ emission occurred at larger distances into their cell and thus escaped detection (as did even some of the $3d \rightarrow 2p$ emission at higher H$^+$ energies, the 3d-state lifetime being 1.5×10^{-8} sec). However, using the fractions of the total H$_\alpha$ emission from the various transitions determined by the other workers (which are all in reasonable accord), the data of Suchannek and Sheridan[18] can be corrected to account for the photons not observed, their data so adjusted being plotted in Fig. 7. As can be seen, these data now agree with the present results[1] at low H$^+$ energies, and with those of Lenormand[12] at higher energies.

For studies of other reactions, Williams et al.[19] used the data of Lenormand[12] for H$^+$ + Ar collisions as a standard to calibrate absolutely their H$_\alpha$ photon detector. They note, however, that "within 2%" the same calibration was obtained when the present data[1] at low energies are used as the standard. In addition, this same detector calibration of Williams et al.[19] was recently used by Yousif et al.[20] to measure total H$_\alpha$ and the $3s \rightarrow 2p$ emission cross sections for 5–100-keV H$^+$ impact on N$_2$ and O$_2$, reactions also investigated here,[21] by Lenormand,[12] and for N$_2$ by Suchannek and Sheridan.[18] When the results of Suchannek and Sheridan[18] are again adjusted (as described above), all these results are in close agreement.

There is thus strong evidence indicating that the present data[1] and those of Lenormand[12] are on a very similar absolute scale, even though they do not directly overlap in H$^+$ energy. This fact has been used in analysis of all the data presented here.

The data of Dawson and Loyd[15] shown in Fig. 7 have been scaled to be 1.88 times their published values, to bring their total H$_\alpha$ emission cross section into accord with the other results. This adjustment also allows the present results and those of Lenormand[12] for the $3s \rightarrow 2p$ emission cross section to be bridged smoothly, providing a pleasing consistancy.

The data of Hughes et al.[14] for Ar targets exhibit features similar to their results for He and Ne targets (and, indeed, for N$_2$ and O$_2$ targets as well). At high H$^+$ energies, these results are fairly close to the other data (typically within about 20%), but diverge to smaller values with decreasing H$^+$ energy. These measurements may have suffered from angular scattering of the fast projectiles moving through the target cell, as opposed to any major differences in photon-detector calibration. Thus, some excited hydrogen atoms produced in the cell may not have traversed the cell's small exit aperture into the photon observation region. This effect would become

more severe with decreasing H$^+$ energy (explaining the different H$^+$ energy dependence of the data), but should not have a large influence on the relative populations of the 3s, 3p, and 3d excited states of hydrogen produced in the collisions (explaining why the fractions of the total H$_\alpha$ emission from these states agree with the other data). This same problem may have affected the measurements of Dawson and Loyd,[15] although the smaller relative H$^+$ energy range covered in their work and the renormalization of their data made here would make this problem much less apparent.

The data for Kr and Xe targets are shown in Figs. 8 and 9, respectively. The data plotted from Dawson and Loyd[15] for Kr targets have again been multiplied by 1.88, this adjustment allowing the results of Lenormand[12] to be smoothly connected to the present data at low H$^+$ energies. Unfortunately, Dawson and Loyd[15] did not investigate Xe targets, but the considerable similarity between these two interactions leaves little doubt that the solid and dashed curves drawn in Fig. 9 should approximate these cross sections.

Some interesting observations can be made by comparing the data for all these reactions. The cross sections for electon capture into the 3s state of hydrogen all reach maxima for H$^+$ energies between 40 keV (for He) and 20 keV (for Xe). In the higher H$^+$ energy range, the fraction of the total H$_\alpha$ emission from the $3s \rightarrow 2p$ transition varies from above 0.9 (for energies beyond 60 keV) to about 0.5 (for energies near 10 keV) for all targets. In the energy range between about 3 and 8 keV covered by Dawson and Loyd,[15] this fraction averages about 0.47 for each of the targets investigated (the fraction expected, as noted earlier, if the 3s, 3p, and 3d excited states were equally populated during the interactions). The present data suggest that this fraction persists (at least approximately) at the lower H$^+$ energies for He and Ne targets.

For Ar, Kr, and Xe targets, however, the $3s \rightarrow 2p$ emission fraction decreases markedly for H$^+$ energies below 3 keV. This energy thus appears by inference to mark the (rather sudden) onset for the complex chemical reactions that give large 3d-excited-state populations[2] at low H$^+$ energies during these interactions.

Unfortunately, fewer data are available to make comparisons for H$_\beta$ emissions from these reactions.[11] However, Dawson and Loyd[15] and Hughes et al.[22] have measured the cross sections for the $4s \rightarrow 2p$ emission in the same respective H$^+$ energy ranges and for the same targets as for H$_\alpha$ emission. In addition, Doughty et al.[23] have measured this emission for all rare-gas-atom targets for H$^+$ energies from 10 to 150 keV. The results of Dawson and Loyd[15] for Ar and Kr targets can again be brought into reasonable agreement with the present data by multiplying them by 1.88. These adjusted results also come into fair agreement with the data of Doughty et al.[23] for these targets (and of Hughes et al.[22] at higher H$^+$ energies for Ar).

For the higher H$^+$ energies, it should also be possible to approximately predict these $4s \rightarrow 2p$ emission cross sections using the n^{-3} scaling law and the data presented above for $3s \rightarrow 2p$ emissions. Such predictions give $4s \rightarrow 2p$ emission cross sections typically only about 20%

larger than Doughty et al.[23] report, a difference within the uncertainties of the measurements. (Use of this scaling law to similarly predict cross sections for electron capture into the $2s$ excited state of hydrogen, incidentally, gives cross sections for He, Ne, and Ar targets in good agreement with such data as obtained by Hughes et al.[24]) Alternately, if one takes the data of Doughty et al.[23] to be exact, the scaling law required would have the dependence $n^{-3.6}$.

However, Lenormand[12] gives data for electron capture into the sum of nl states at the $n = 3$ and 4 levels, and reports that the relative cross-section magnitudes suggest a dependence on n between n^{-2} and $n^{-2.5}$. (The difference in such cross section ratios for an n^{-3} or $n^{-2.5}$ scaling law is only about 15%, again on the order of the uncer-

tainties in the photon-detector calibrations used at the H_α and H_β wavelengths.) In addition, because these data include electron capture into np and nd states, the n^{-3} scaling law may not be valid. Indeed, if modified forms[6] of the scaling laws for np and nd states are applied to these data of Lenormand,[12] a less strong dependence than n^{-3} would be expected.

ACKNOWLEDGMENTS

[1]B. Van Zyl, H. L. Rothwell, Jr., and H. Neumann, Phys. Rev. A 21, 730 (1980).

[2]Although the emission components from the $np \rightarrow 2s$ and $nd \rightarrow 2p$ transitions could not be separated experimentally, most of these emissions probably come from $nd \rightarrow 2p$ transitions because of the small branching ratio (~ 0.12) for $np \rightarrow 2s$ decay.

[3]B. Van Zyl, H. Neumann, H. L. Rothwell, Jr., and R. C. Amme, Phys. Rev. A 21, 716 (1980).

[4]B. Van Zyl, G. H. Dunn, G. Chamberlain, and D. W. O. Heddle, Phys. Rev. A 22, 1916 (1980).

[5]B. Van Zyl, M. W. Gealy, and H. Neumann, Phys. Rev. A 28, 176 (1983).

[6]B. Van Zyl, M. W. Gealy, and H. Neumann, Phys. Rev. A 31, 2922 (1985).

[7]D. Rapp and W. E. Francis, J. Chem. Phys. 37, 2631 (1962).

[8]These data are total-emission polarizations. Because the emissions from excited ns states will not be polarized, the $np \rightarrow 2s$ and $nd \rightarrow 2p$ emissions must be more polarized than the data shown.

[9]U. Fano and J. H. Macek, Rev. Mod. Phys. 45, 553 (1973). According to this work, the polarizations of the radiations from the $m_l = 0$, ± 1, and ± 2 substates of nd states should be $+0.48$, $+0.26$, and -0.70, respectively.

[10]D. H. Jaecks (private communication). These results can be found in P. J. Martin, Ph.D. thesis, University of Nebraska, 1975.

[11]Most workers report cross sections $\sigma_{ec}(nl)$ for electron capture into the nl excited states of hydrogen. The emission cross

sections are thus determined from $\sigma_{em}(H_\alpha)$ $= \sigma_{ec}(3s) + 0.118\sigma_{ec}(3p) + \sigma_{ec}(3d)$ and $\sigma_{em}(H_\beta) = 0.584\sigma_{ec}(4s)$ $+ 0.119\sigma_{ec}(4p) + 0.746\sigma_{ec}(4d)$.

[12]J. Lenormand, J. Phys. (Paris) 37, 699 (1976).

[13]J. C. Ford and E. W. Thomas, Phys. Rev. A 5, 1694 (1972).

[14]R. H. Hughes, C. A. Stigers, B. M. Doughty, and E. D. Stokes, Phys. Rev. A 1, 1424 (1970).

[15]H. R. Dawson and D. H. Loyd, Phys. Rev. A 9, 166 (1974); 15, 43 (1977).

[16]R. H. Hughes, H. R. Dawson, B. M. Doughty, D. B. Kay, and C. A. Stigers, Phys. Rev. 146, 53 (1966).

[17]H. R. Dawson (private communication).

[18]R. G. Suchannek and J. R. Sheridan, Geophys. Res. Lett. 2, 247 (1975).

[19]I. D. Williams, J. Geddes, and H. B. Gilbody, J. Phys. B 15, 1377 (1982).

[20]F. Yousif, J. Geddes, and H. B. Gilbody, in Proceedings of the Fourteenth International Conference on the Physics of Electronic and Atomic Collisions, edited by M. J. Coggiola, D. L. Huestis, and R. P. Saxon (Stanford University, Palo Alto, 1985), p. 580.

[21]B. Van Zyl and H. Neumann, J. Geophys. Res. 85, 6006 (1980).

[22]R. H. Hughes, H. R. Dawson, and B. M. Doughty, Phys. Rev. 164, 166 (1967).

[23]B. M. Doughty, M. L. Goad, and R. W. Cernosek, Phys. Rev. A 18, 29 (1978).

[24]R. H. Hughes, E. D. Stokes, S. S. Choe, and T. J. King, Phys. Rev. A 4, 1453 (1971).